

PAPER • OPEN ACCESS

## Quasiparticle formulation of a multiphonon method and its application to the $^{20}\text{O}$ nucleus

To cite this article: P. Veselý *et al* 2018 *J. Phys.: Conf. Ser.* **966** 012047

View the [article online](#) for updates and enhancements.

# Quasiparticle formulation of a multiphonon method and its application to the $^{20}\text{O}$ nucleus

P. Veselý<sup>1</sup>, G. De Gregorio<sup>1,2,3</sup>, F. Knapp<sup>4</sup>, N. Lo Iudice<sup>2,3</sup>

<sup>1</sup>Nuclear Physics Institute, Czech Academy of Sciences, 250 68 Řež, Czech Republic

<sup>2</sup>Dipartimento di Fisica, Università di Napoli Federico II, Naples, Italy

<sup>3</sup>INFN Sezione di Napoli, Naples, Italy

<sup>4</sup>Faculty of Mathematics and Physics, Charles University, Prague, Czech Republic

E-mail: p.vesely@ujf.cas.cz

**Abstract.** We outline briefly the quasiparticle formulation of a microscopic multiphonon approach known as equation of motion phonon method and discuss its application to the neutron rich semi-magic  $^{20}\text{O}$ . Our calculation emphasizes the crucial role of the two-phonon configurations, responsible for establishing an almost one to one correspondence between theoretical and experimental energy levels and for fragmenting the dipole strength, in qualitative agreement with the data. In particular, the fragmentation yields two dipole levels below the neutron threshold which correspond to the two peaks recently observed.

## 1. Introduction

The equations of motion phonon method (EMPM) was developed few years ago [1, 2, 3]. It derives and solves iteratively a set of equations of motion to generate an orthonormal basis of multiphonon states built of phonons obtained in Tamm-Dancoff approximation (TDA). The basis so obtained is then adopted to diagonalize the residual Hamiltonian in a multiphonon space. The formalism treats one-phonon as well as multiphonon states on the same footing, takes into account the Pauli principle, and holds for any Hamiltonian.

The method was originally derived in the particle-hole scheme and applied to describe the dipole response in the heavy neutron rich nuclei  $^{208}\text{Pb}$  [4] and  $^{132}\text{Sn}$  [5]. Recently, it was formulated in terms of Bogoliubov quasiparticles and applied to the open-shell  $^{20}\text{O}$  [6]. Among the neutron rich oxygen isotopes,  $^{20}\text{O}$  is one of the most extensively studied.

Several experiments have yielded a rich spectrum [7, 8, 9, 10]. Electromagnetic excitations induced by heavy-ion collisions have determined the dipole cross section over a wide energy range [11], while a virtual-photon scattering experiment have detected two  $1^-$  levels below the neutron decay threshold [12, 13]. These two excitations were further investigated in two recent experiments using ( $^{20}\text{O} + \alpha$ ) and ( $^{20}\text{O} + \text{Au}$ ) probes [14].

The low-lying spectra of  $^{20}\text{O}$  were investigated theoretically within the coupled-cluster (CC) theory [15] and an extended shell-model using chiral two- and three-body interactions up to third order [15, 16, 17, 18]. The dipole strength distribution was studied within the phenomenological Shell-Model [19], relativistic RPA [20], time-dependent HF (TDHF) [21], and RPA plus PVC [22]. The objective of these studies was to establish if the low-lying peaks are a manifestation of the pygmy dipole resonance (PDR) or are simply single particle excitations.



Both spectrum and dipole response are investigated here in a unified fashion within the EMPM.

## 2. EMPM in the quasiparticle formalism

The main goal of the EMPM is to generate recursively a basis of  $n$ -phonon ( $n = 0, 1, 2, \dots$ ) states  $|\alpha_n\rangle$ , of energy  $E_{\alpha_n}$ , having the form

$$|\alpha_n\rangle = \sum_{\lambda\alpha} C_{\lambda\alpha_{n-1}}^{\alpha_n} |(\lambda \times \alpha_{n-1})^{\alpha_n}\rangle = \sum_{\lambda\alpha} C_{\lambda\alpha_{n-1}}^{\alpha_n} \left\{ O_{\lambda}^{\dagger} \times |\alpha_{n-1}\rangle \right\}^{\beta_n}, \quad (1)$$

where

$$O_{\lambda}^{\dagger} = \sum_{r \leq s} c_{rs}^{\lambda} Z_{rs}^{\lambda} = - \sum_{r \leq s} c_{rs}^{\lambda} \zeta_{rs} (\alpha_r^{\dagger} \times \alpha_s^{\dagger})^{\lambda} \quad (2)$$

is the quasiparticle TDA phonon operator of energy  $E_{\lambda}$  acting on the  $(n-1)$ -phonon states  $|\alpha_{n-1}\rangle$  of energies  $E_{\alpha_{n-1}}$ , assumed to be known. The normalization factor  $\zeta_{rs} = (1 + \delta_{rs})^{-1/2}$  has been used.

We start with constructing the equations of motion

$$\langle \beta | [H, O_{\lambda}^{\dagger}] | \alpha \rangle = (E_{\beta} - E_{\alpha}) \langle \beta | O_{\lambda}^{\dagger} | \alpha \rangle, \quad (3)$$

where the subscript  $n$  was omitted for simplicity. After expanding the commutator and expressing the quasiparticle operators  $Z_{rs}^{\lambda}$  in terms of the phonon operators by inverting Eq. (2), we obtain [6] the generalized eigenvalue equations

$$\sum_{\lambda'\alpha'\lambda_1\alpha_1} \left[ (E_{\lambda} + E_{\alpha}) \delta_{\lambda\lambda_1} \delta_{\alpha\alpha_1} + \mathcal{V}_{\lambda\alpha, \lambda_1\alpha_1}^{\beta} \right] \mathcal{D}^{\beta}(\lambda_1\alpha_1, \lambda'\alpha') C_{\lambda'\alpha'}^{\beta} = E_{\beta} \sum_{\lambda'\alpha'} \mathcal{D}^{\beta}(\lambda\alpha, \lambda'\alpha') C_{\lambda'\alpha'}^{\beta}. \quad (4)$$

Here

$$\mathcal{D}^{\beta}(\lambda\alpha, \lambda'\alpha') = \langle (\lambda \times \alpha)^{\beta} | (\lambda' \times \alpha')^{\beta} \rangle \quad (5)$$

is the overlap or metric matrix and  $\mathcal{V}^{\beta}$  is a phonon-phonon potential of the simple form

$$\mathcal{V}^{\beta}(\lambda\alpha, \lambda_1\alpha_1) = \sum_{\sigma} W(\beta\lambda_1\alpha\sigma; \alpha_1\lambda) \mathcal{V}_{\lambda\alpha, \lambda_1\alpha_1}^{\sigma}, \quad (6)$$

where  $W$  is a Racah coefficient and

$$\mathcal{V}_{\lambda\alpha, \lambda_1\alpha_1}^{\sigma} = \frac{1}{2} \sum_{rtsq} \rho_{\lambda\lambda_1}([r \times t]^{\sigma}) \mathcal{V}_{rtsq}^{\sigma} \rho_{\alpha\alpha_1}^{(n-1)}([s \times q]^{\sigma}). \quad (7)$$

The quantities  $\rho_{\lambda\lambda_1}([r \times t]^{\sigma})$  and  $\rho_{\alpha\alpha_1}^{(n-1)}([s \times q]^{\sigma})$  denote, respectively, the TDA ( $n=1$ ) and the  $n$ -phonon ( $n > 1$ ) density matrices [6], while  $\mathcal{V}_{rtsq}^{\sigma}$  (22) are the quasiparticle matrix elements. Their expressions can be found in Ref. [6].

The generalized eigenvalue problem (4) is formulated in terms of the over-complete set of states  $|\lambda \times \alpha_{n-1}\rangle^{\alpha_n}$ . A procedure based on the Cholesky decomposition method enables us to extract a basis of linearly independent eigenstates and to turn the singular eigenvalue equation (4) into a regular one [1]. This new equation is solved iteratively starting from the TDA phonons  $|\alpha_1 = \lambda\rangle$  to yield an orthonormal multiphonon basis  $\{|0\rangle, |\alpha_1\rangle, \dots, |\alpha_n\rangle, \dots\}$ .

The basis so obtained can be adopted to solve the eigenvalue equations in the multiphonon space

$$\sum_{n'\beta_{n'}} \left[ (E_{\alpha_n} - \mathcal{E}_{\nu}) \delta_{n'n'} \delta_{\alpha_n\beta_{n'}} + \mathcal{V}_{\alpha_n\beta_{n'}} \right] \mathcal{C}_{\beta_{n'}}^{(\nu)} = 0, \quad (8)$$

where the potential

$$\mathcal{V}_{\alpha_n \beta_{n'}} = \delta_{n'(n+1)} \mathcal{V}_{\alpha_n \beta_{n'}} + \delta_{n'(n+2)} \mathcal{V}_{\alpha_n \beta_{n'}} \quad (9)$$

couples subspaces differing by one and two phonons for a two-body Hamiltonian.

The solution of the above equations yields the final eigenfunctions

$$|\Psi_\nu\rangle = \sum_{\alpha_n} C_{\alpha_n}^{(\nu)} |\alpha_n\rangle, \quad (10)$$

where  $|\alpha_n\rangle$  are the correlated  $n$ -phonon states of the form (1).

### 3. Calculations and results

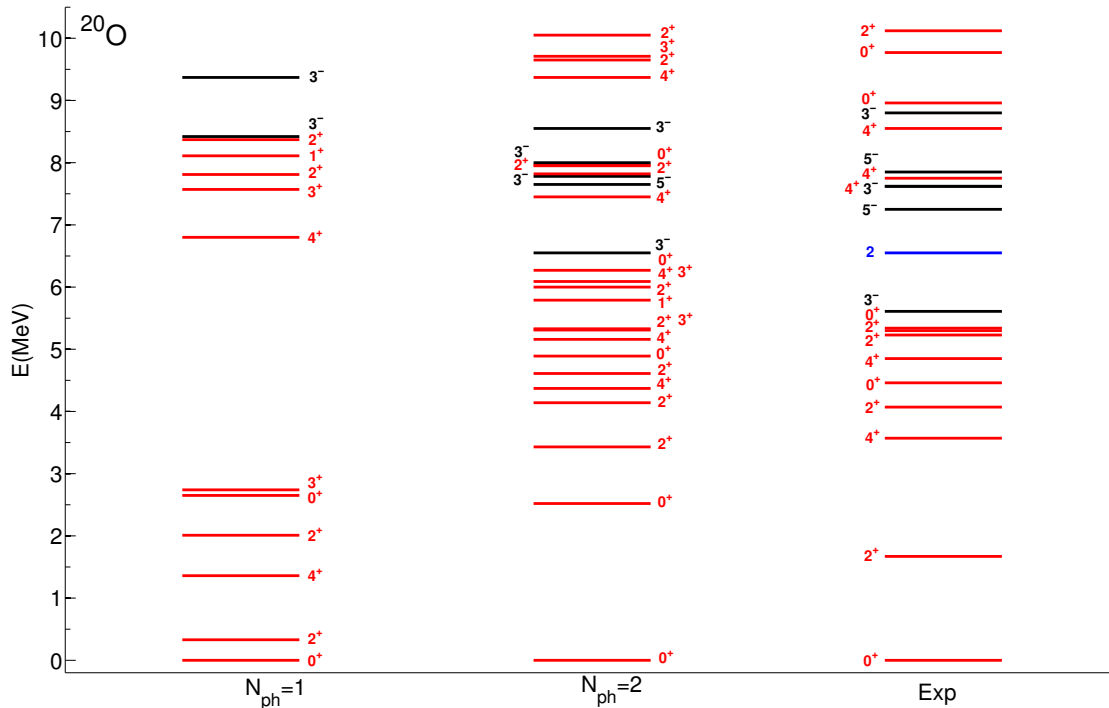


**Figure 1.** Theoretical versus experimental energy levels in  $^{20}\text{O}$  (from [6]).

We used the nucleon-nucleon optimized chiral potential  $\text{NNLO}_{\text{opt}}$  whose parameters were determined by a new optimization method which minimizes the effects of the three-nucleon force [23].

A canonical HFB basis [24] was generated in the configuration space of 11 harmonic oscillator major shells up to the principal quantum number  $N_{\text{max}} = 10$ . The TDA phonons were determined in smaller configuration space which included up to the  $pfh$  major shell. Their energy and structure did not change when the full space up to  $N_{\text{max}} = 10$  was used. A procedure exploiting the Gram-Schmidt orthogonalization method enabled us to generate phonons free of the spurious admixtures induced by the center of mass motion and the particle-number violation [24].

We built a multiphonon basis up to  $n = 2$  and included all two-phonon configurations fulfilling the condition  $E_{\lambda_1} + E_{\lambda_2} \leq 30$  MeV. This cut-off was fixed so as to reproduce roughly the first excited  $1^-$  level. The cut-off affects only the energy of the correlated ground state but leaves unchanged the separation energies between excited levels. It would be necessary to include the

three-phonon states in a space large enough to restore the correct separation between excited and ground state energies. These configurations are known to couple strongly to the one-phonon states and to push them down in energy [3]. Though feasible in principle, the inclusion of a large number of three-phonon states would have required unbearably lengthy calculations unless we resorted to some efficient approximations. We plan to do this in the future.

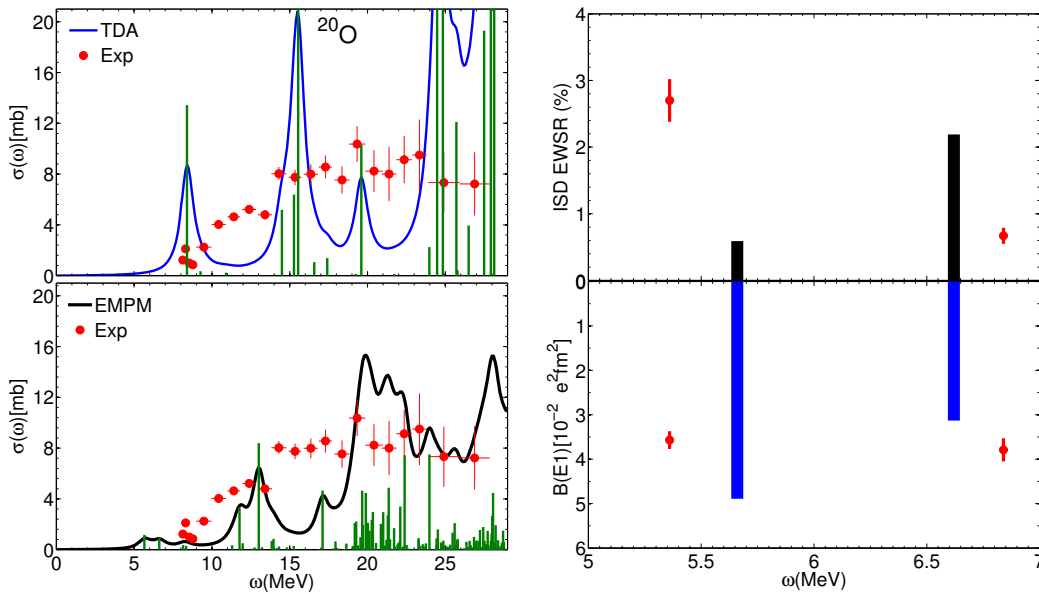


**Figure 2.** Theoretical and experimental dipole cross sections are plotted on the left. The isoscalar and isovector dipole transition strengths collected by the lowest two  $1^-$  states are compared with recent data on the right.

Theoretical versus experimental [7, 8, 9, 10] spectra are shown in Figure 1. A satisfactory agreement between theory and experiments is achieved only once the two phonons are included. Indeed, they produce a much richer spectrum and redistribute the energies so that an almost one to one correspondence between theoretical and experimental energy levels is achieved.

The two-phonon configurations play a crucial role also in shaping the dipole cross section. As shown in Figure 2, the phonon coupling induces a severe fragmentation of the strength and a consequent quenching and spreading of the single peaks, consistently with the data. Appreciable discrepancies are noticeable, however in the low-energy region, where the experimental cross section is seriously underestimated. In fact, the strength collected by all the states up to  $\sim 15$  MeV accounts only for  $\sim 6\%$  of the TRK sum rule, just half the  $\sim 12\%$  fraction estimated experimentally [11, 12, 13]. The cross section integrated up to  $\sim 27$  MeV accounts for  $\sim 38\%$  of the TRK sum rule to be compared with the  $\sim 45\%$  determined experimentally.

Another intriguing effect of the phonon coupling is observed at low-energy. The lowest TDA  $1^-$  peak gets fragmented into several smaller peaks with the appearance of two levels below the neutron decay threshold in agreement with the data obtained in a virtual-photon scattering experiment performed at MSU [12, 13] at around 100 MeV/nucleon. The isovector transition strengths measured by those experiments were reproduced with great accuracy by our calculation[6].

Very recently, a new measurement [14] using the ( $^{20}\text{O} + \alpha$ ) and ( $^{20}\text{O} + \text{Au}$ ) probes produced for these two levels the isoscalar dipole (ISD) strengths and, in addition, new isovector transition

probabilities which differ appreciably from the previous measurements [12, 13]. The agreement with the theoretical isovector strengths is slightly spoiled but still satisfactory. Concerning the ISD transitions, the calculation reproduces the overall strength. In fact, the two levels are estimated to exhaust 2.78 % of the energy weighted sum rule (EWSR), almost within the experimental errors of the measured value. However, it is distributed among the two levels just in the opposite way.

These two low-lying  $1^-$  states have a dominant two-phonon character. The one-phonon components, responsible for the transition, account for 10% of the lower state and for 20% of the one at higher energy. A level crossing would be desirable. This may be induced for instance by the inclusion of the three-phonon configurations.

#### 4. Conclusions

We have seen that the quasiparticle formulation keeps the same simplicity of EMPM in the particle-hole scheme and is well suited for clarifying the role of complex configurations on the properties of open shell nuclei, including those far from the stability line. The neutron-rich  $^{20}\text{O}$  isotope is an important illustrative example. For the study of this nucleus, we have performed a calculation in a truncated space including up to a fraction of two-phonon states. The truncation of the two-phonon configurations is the only free parameter of our calculation. It was dictated by the necessity of keeping a reasonable energy gap between the excited and correlated ground states.

A calculation in the two-phonon space, while affecting little the excited states, would have depressed very significantly the ground state. It would have been, therefore, necessary to restore the correct energy gap by including a sufficiently large number of three-phonon states, which are known to couple strongly to the one-phonon configurations and to push the excited states down in energy. While feasible, the inclusion of the three phonon states would require a more efficient numerical implementation of EMPM. We plan to cope with this task in the future.

Although limited to a truncated space, the calculation has shown that the two-phonon configurations have a very strong impact on the spectra and the dipole response. They improve greatly the agreement between theoretical and experimental spectra by enhancing the levels density and redistributing the TDA energies, provide a fairly satisfactory description of the cross section in the region of the giant dipole resonance in virtue of the strong fragmentation of the dipole strength induced by the phonon coupling. They are also responsible for the appearance of two  $1^-$  levels below the neutron threshold, detected in recent experiments, and reproduce the overall strength measured for these two levels.

#### Acknowledgments

This work was partly supported by the Czech Science Foundation (P203-13-07117S). Two of the authors (F.K. and P.V.) thank the Istituto Nazionale di Fisica Nucleare (Italy) for financial support. Highly appreciated was the access to computing and storage facilities provided by the Meta Centrum under Program No. LM2010005 and the CERITSC under the program Centre CERIT Scientific Cloud, part of the Operational Program Research and Development for Innovations, Register No. CZ.1.05/3.2.00/08.0144.

#### References

- [1] Andreozzi F, Knapp F, Lo Iudice N, Porrino A and Kvasil J 2007 *Phys. Rev. C* **75** 044312
- [2] Andreozzi F, Knapp F, Lo Iudice N, Porrino A and Kvasil J 2008 *Phys. Rev. C* **78** 054308
- [3] Bianco D, Knapp F, Lo Iudice N, Andreozzi F, and Porrino A 2012 *Phys. Rev. C* **85** 014313
- [4] Knapp F, Lo Iudice N, Veselý P, Andreozzi F, De Gregorio G and Porrino A 2014 *Phys. Rev. C* **90** 014310
- [5] Knapp F, Lo Iudice N, Veselý P, Andreozzi F, De Gregorio G and Porrino A 2015 *Phys. Rev. C* **92** 054315
- [6] De Gregorio G, Knapp F, Lo Iudice N and Veselý P 2016 *Phys. Rev. C* **93** 044314
- [7] Tilley D R, Cheves C M, Kelley J H, Raman S and Weller H R 1998 *Nucl. Phys. A* **636** 249

- [8] Jewell J K, Riley L A, Cottle P D, Kemper K W, Glasmacher T, Ibbotson R W, Scheit H, Chromik M, Blumenfeld Y, Hirzebruch S E, Marechal F and Suomijarvi T 1999 *Phys. Lett. B* **454** 181
- [9] Khan E, Blumenfeld Y, Van Giai N, Suomijarvi T, Alamanos N, Auger F, Colo G, Frascaria N, Gillibert A, Glasmacher T, Godwin M, Kemper K W, Lapoux V, Lhenry I, Marechal F, Morrissey D J, Musumarra A, Orr N A, Ottini-Hustache S, Piattelli P, Pollacco E C, Roussel-Chomaz P, Roynette J C, Santonocito D, Sauvestre J E, Scarpaci J A and Volpe C 2000 *Phys. Lett. B* **490** 45
- [10] Stanoiu M et al 2004 *Phys. Rev. C* **69** 034312
- [11] Leistenschneider A et al 2001 *Phys. Rev. Lett.* **86** 5442
- [12] Tryggestad E, Aumann T, Baumann T, Bazin D, Beene J R, Blumenfeld Y, Brown B A, Chartier M, Halbert M L, Heckman P, Liang J F, Radford D C, Shapira D, Thoennessen M and Varner R L 2002 *Phys. Lett. B* **541** 52
- [13] Tryggestad E, Baumann T, Heckman P, Thoennessen M, Aumann T, Bazin D, Blumenfeld Y, Beene J R, Lewis T A, Radford D C, Shapira D, Varner R L, Chartier M, Halbert M L and Liang J F 2003 *Phys. Rev. C* **67** 064309
- [14] Nakatsuka N et al 2017 *Phys. Lett. B* **768** 387
- [15] Jansen G R, Engel J, Hagen G, Navrátil P and Signoracci A 2014 *Phys. Rev. Lett.* **113** 142502
- [16] Jensen O, Hagen G, Hjorth-Jensen M, Brown B A and Gade A 2011 *Phys. Rev. Lett.* **107** 032501
- [17] Hagen G, Hjorth-Jensen M, Jansen G R, Machleidt R and Papenbrock T 2012 *Phys. Rev. Lett.* **108** 242501
- [18] Holt J D, Menendez J and Schwenk A 2013 *Eur. Phys. J. A* **49** 39
- [19] Sagawa H and Suzuki T 1999 *Phys. Rev. C* **59** 3116
- [20] Vretenar D, Paar N, Ring P and Lalazissis G A 2001 *Nucl. Phys. A* **692** 496
- [21] Tohyama M and Umar A S 2001 *Phys. Lett. B* **516** 415
- [22] Colò G and Bortignon P F 2001 *Nucl. Phys. A* **696** 427
- [23] Ekstroem A, Baardsen G, Forssen C, Hagen G, Hjorth-Jensen M, Jansen G R, Machleidt R, Nazarewicz W, Papenbrock T, Sarich J and Wild S M 2013 *Phys. Rev. Lett.* **110** 192502
- [24] Bianco D, F Knapp F, Lo Iudice N, Veselý P, Andreozzi F, De Gregorio G and Porrino 2014 *J. Phys. G: Nucl. Part. Phys.* **41** 025109